DOI: 10.1051/epjconf/201714611043

Measurements of cross sections for the ^{209}Bi(n, 4n) reaction by using high energy neutrons with continuous energy spectra

Kyung Joo Min[1], Sang-In Bak[1], Cheolmin Ham[1], Eun Jin In[1], Do Yoon Kim[1], Hyunjeong Myung[2], Chungbo Shim[2], Jae Won Shin[3], Yujie Zhou[1], Tae-Sun Park[2], Seung-Woo Hong[2,a], and V.N. Bhoraskar[4]

[1] Department of Energy Science, Sungkyunkwan University, Suwon, Korea
[2] Department of Physics, Sungkyunkwan University, Suwon, Korea
[3] Department of Physics, Soongsil University, Seoul, Korea
[4] Department of Physics, S. P. Pune University, Pune, India

Abstract. We measured ^{209}Bi(n, 4n) cross sections at neutron energies $E_n = 29.8 \pm 1.8$ MeV and $E_n = 34.8 \pm 1.8$ MeV. Bismuth oxide samples were irradiated with the neutrons produced by impinging 30, 35 and 40 MeV proton beams on a 1.05 cm thick beryllium target, where the proton beams were from the MC-50 Cyclotron of Korea Institute of Radiological Medical Sciences (KIRAMS). The neutron flux for each proton beam energy E_p, $\Phi_{E_p}(E_n)$, has a broad spectrum with respect to E_n. By taking the difference in the neutron fluxes, the difference spectra, $\Phi_{40}(E_n) - \Phi_{35}(E_n)$ and $\Phi_{35}(E_n) - \Phi_{30}(E_n)$, are obatined and found to be peaked at $E_n = 29.8$ and 34.8 MeV, respectively, with a width of about 3.6 MeV. By making use of this observation and employing the TENDL-2009 library we could extract the ^{209}Bi(n, 4n)^{206}Bi cross sections at the aforementioned neutron energies.

1. Introduction

Accurate cross sections for ^{209}Bi(n, xn) are needed for the development of Accelerator Driven Systems with Pb-Bi coolants [1,2], while the experimental data are scarce. Recently the cross sections have been measured by the activation method in the tens of MeV region, by using the quasi mono-energetic neutrons obtained by the ^{7}Li(p, n)^{7}Be reaction [3–7].

We report on our measurements of the ^{209}Bi(n, 4n)^{206}Bi cross sections done by the activation method, where we have used the neurtons obtained by impinging 30, 35 and 40 MeV proton beams on a thick beryllium target. The neutron spectrum for each proton beam energy is not mono-energetic but broad with respect to the neutron energy E_n. But the difference of two spectra with adjacent proton energies is observed to have a peak structure with some width, which enables us to extract the cross sections at $E_n = (29.8 \pm 1.8)$ MeV and (34.8 ± 1.8) MeV.

2. GEANT4 simulations of neutron flux and cross section measurements

The experimental work was carried out by using the MC-50 Cyclotron [8] at Korea Institute of Radiological Medical Science (KIRAMS), which is capable of providing proton beams of energy $(20 \sim 50)$ MeV with 5 MeV intervals. The overall layout of our experiment is given in Fig. 1 of Ref. [9]. Neutrons were produced by directing 30, 35 and 40 MeV proton beams of 20μA to a beryllium target of thickness 1.05 cm. A neutron collimator was installed downstream along the neutron beam after the beryllium target, and the samples were placed 100 cm away from the end of the collimator.

In [9] simulations for the neutron spectra scored at the sample position was conducted. We adopted the simulation results of the neutron spectra given in [9], where the GEANT4 code v10.0 [10] was used with the newly developed hadronic model [11] that takes the ENDF/B-VII.1 data for the ^{9}Be(p, n)^{9}B cross section. The angular dependence of the neutron spectra is almost independent of angles when $\theta < 5^\circ$, where θ is the angle of the neutron momentum with respect to the proton beam axis. Figure 1 shows the neutron spectra for 30, 35 and 40 MeV protons with the beam current 20 μA [9]. The neutrons were scored at $0^\circ \leq \theta \leq 1.6^\circ$, and we put our samples within these angles. Here we note that a validity test of the simulated neutron fluxes has been done [9] by measuring the integrated activities of ^{56}Mn and ^{24}Na produced by the reactions ^{56}Fe(n, p)^{56}Mn and ^{27}Al(n, α)^{24}Na, respectively, and they were found to be in agreement with the data with $\sim 20\%$ uncertainty.

We used three sets of bismuth and niobium samples, and each of them consisted of about 3.04 grams of bismuth oxide powder of purity 99.9% and 3.02 grams of niobium powder of purity 99.99%. The niobium powders were used for the purpose of monitoring the neutron fluence. All the samples were placed at a distance of 100 cm from the end of the collimator assembly, and their positions are adjusted to satisfy the condition of $\theta \leq 1.6^\circ$. The samples were irradiated for 90 minutes. After the irradiation the gamma-ray activities from the irradiated samples were measured by a carefully shielded HPGe detector coupled with a 8K multi channel analyzer. The detector was calibrated with a standard source which contains ^{60}Co, ^{133}Ba, ^{137}Cs, ^{155}Eu,

[a] e-mail: swhong@skku.ac.kr

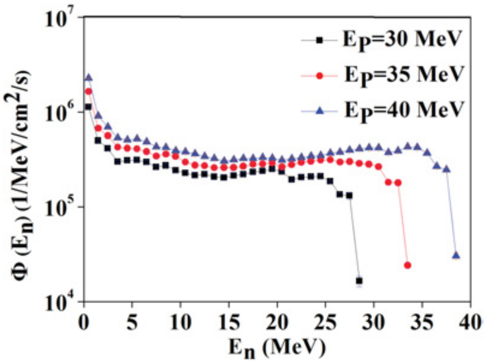

Figure 1. GEANT4 simulations of energy distribution of neutrons produced by 30, 35 and 40 MeV protons of 20 μA. Neutrons are scored at $0^\circ \leq \theta \leq 1.6^\circ$ [9].

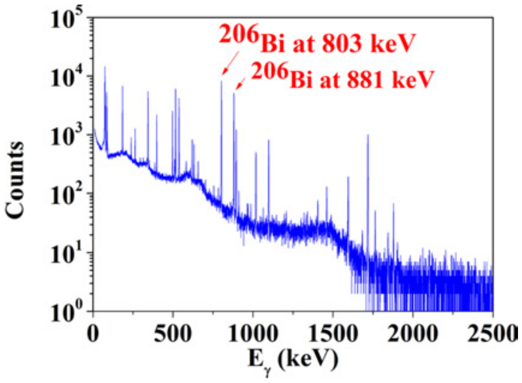

Figure 2. Gamma-ray spectrum from the bismuth sample irradiated by neutrons generated by the 40 MeV 20 μA proton beam. Two major gamma peaks from ^{206}Bi are indicated.

^{154}Eu and ^{152}Eu isotopes. Figure 2 shows the gamma-ray spectrum from the irradiated bismuth sample taken for 24 hours. The daughter nuclide ^{206}Bi has $T_{1/2} = 6.24$ d, and emits gamma-rays of energies $E_\gamma = 803$ keV ($I_\gamma = 99\%$) and 881 keV ($I_\gamma = 66.2\%$).

3. Methods

The experiment was done by using a neutron activation method. After the neutron irradiation and measuring the gamma-ray spectra, the area of a photo-peak (A) at $T = T_{IR} + T_{CO} + T_{CL}$ in the gamma-ray spectrum reads [12]

$$A = \frac{N}{\lambda}\varepsilon\beta\left(1 - e^{-\lambda T_{IR}}\right)e^{-\lambda T_{CO}}\left(1 - e^{-\lambda T_{CL}}\right)\frac{T_{AT}}{T_{CL}}\hat{A},$$
$$\hat{A} \equiv \int \sigma(E_n)\Phi(E_n)dE_n, \qquad (1)$$

where $\sigma(E_n)$ is the cross section of the neutron induced reaction at neutron energy E_n, $\Phi(E_n)$ is the neuron flux of energy E_n, λ is the decay constant of the daughter nuclide, N is the number of atoms in the sample, ε is the efficiency of the detector, β is the branching ratio of daughter nuclide, T_{IR} is the irradiation time, T_{CO} is the cooling time, T_{AT} is the actual measurement time and T_{CL} is the clock measurement time, so that the factor $\frac{T_{AT}}{T_{CL}}$ is for dead time correction.

As seen in Fig. 1, the neutron spectrum for a given proton energy is broad and continuous. Note that at the neutron energies higher than $\sim$ 10 MeV, each neutron

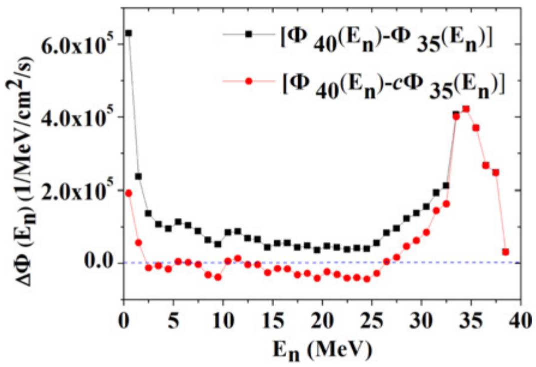

Figure 3. The subtracted neutron flux with (red circles) and without (black squares) the flux cancellation factor is plotted as a function of neutron energy.

spectrum remains more or less constant in magnitude and then rapidly drops to zero. This feature enables us to use the subtraction method [13], which utilizes the observation that the difference of two neutron spectra with neighboring proton energies can be viewed as "quasi mono-energetic" neutron beams with a non-vanishing but small width. For example, let us define a quantity $\Delta\Phi_{40:35}(E_n)$ by

$$\Delta\Phi_{40:35}(E_n) \equiv \Phi_{40}(E_n) - c\Phi_{35}(E_n), \qquad (2)$$

where the subscripts denote the proton energies in MeV. $\Phi_{40}(E_n)$ is bigger than $\Phi_{35}(E_n)$ in the plateau region and thus c is introduced to make $\int_{E_{th}}^{E} \Delta\Phi_{40:35}(E_n)\,dE_n = 0$. We find c to be 1.27. The relevant neutron energy region is from $\sim$ 22.5 MeV to $\sim$ 39 MeV, where 22.5 MeV is the threshold energy for ^{209}Bi(n, 4n)^{206}Bi reaction and 39 MeV is the highest neutron energy.

$\Delta\Phi_{40:35}(E_n)$ is plotted in Fig. 3, which shows a quasi mono-energetic peak of neutrons at high energies. By fitting the peak at high energies to a Gaussian function, we found the peak of $\Delta\Phi_{40:35}(E_n)$ is centered at E_n = 34.8 MeV with a width of 3.6 MeV. We also evaluated the flux-weighted mean energy

$$\langle E_n\rangle \equiv \frac{\int_{E_c}^{39} E_n\,\Delta\Phi_{40:35}(E_n)\,dE_n}{\int_{E_c}^{39} \Delta\Phi_{40:35}(E_n)\,dE_n}, \qquad (3)$$

which gives us $\langle E_n\rangle = 34.8 \pm 1.8$ MeV where E_c is taken as 31 MeV. We can thus extract the mean value of the cross section in the interval [E_c, 39 MeV] by using the following expression, where A_{35} and A_{40} are the activities at the end of the irradiation of ^{206}Bi obtained by 35 and 40 MeV protons.

$$\bar{\sigma} = \frac{\frac{A_{40} - cA_{35}}{N(1-e^{-\lambda T_{IR}})} - \int_{E_{th}}^{E_c} \sigma(E_n)\Delta\Phi_{40:35}(E_n)\,dE_n}{\int_{E_c}^{39} \Delta\Phi_{40:35}(E_n)\,dE_n} \qquad (4)$$

We take this as the cross section at a neutron energy $E_n = 34.8 \pm 1.8$ MeV. We extract the cross section at $E_n = 29.8 \pm 1.8$ MeV in a similar way.

4. Results

To extract the value of $\bar{\sigma}$ from Eq. (4), we need to first evaluate the integral in the numerator of Eq. (4). For this, we adopted the evaluated nuclear data TENDL-2009

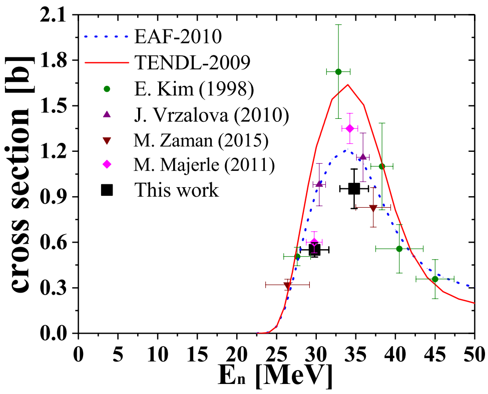

Figure 4. ^{209}Bi(n, 4n)^{206}Bi cross sections. The solid line is TENDL-2009 library, the empty points are experiment data and the filled ones are our preliminary results.

library [14] for $\sigma(E_n)$ in the integral. Since the difference spectra $\Delta\Phi_{40:35}(E_n)$ is small in this low-energy region, the dependence of our results on the library turned out to be not so significant. The cross section obtained in this procedure is $\bar{\sigma} = (953 \pm 129)$ mb at $E_n = (34.8 \pm 1.8)$ MeV, where the error bar of the cross section is mainly due to the uncertainty in the neutron fluence and the above mentioned dependence on the adopted library for the low-energy contributions. A similar analysis with neutron flux $\Phi_{35}(E_n)$ and $\Phi_{30}(E_n)$ at $E_p = 35$ and 30 MeV, respectively, gave us $c \simeq 1.34$ and $\bar{\sigma} = (550 \pm 47)$ mb at $E_n = (29.8 \pm 1.8)$ MeV. The resulting cross sections for the ^{209}Bi(n, 4n)^{206}Bi reaction are plotted in Fig. 4, where the solid line repsresents the cross sections from the TENDL-2009 library, the empty triangles and squares are the existing experimental data [3,15], and our results are depicted by the filled circles. Our experimental cross sections do not agree well with the calculated cross sections, and re-measurements will be carried out in the future.

5. Summary

We measured ^{209}Bi(n, 4n)^{206}Bi cross sections with high energy neutrons. The bismuth oxide samples were irradiated with neutrons generated by 30, 35 and 40 MeV protons of 20 μA with 1.05 cm thick beryllium target. After the irradiation the activities of the irradiated samples were measured by a HPGe detector. In the analysis, we used the neutron flux generated by 30, 35 and 40 MeV protons at 20 μA on a thick beryllium target, which we simulated by the GEANT4. The simulated neutron flux is more or less constant in magnitude and drops sharply. Based on these features, a subtraction method was used to extract the average cross sections. The subtracted flux was fitted by a Gaussian curve, and the central values and width of the Gaussian curves were taken as the neutron energies and their errors, respectively. The cross section of ^{209}Bi(n, 4n)^{206}Bi is obtained as (550 ± 47) mb at $E_n = (29.8 \pm 1.8)$ MeV and (953 ± 129) mb at $E_n = (34.8 \pm 1.8)$ MeV. Our experiments and analysis showed that continuous neutron spectra could be used for extracting the neutron induced cross sections.

This work was supported in part by the Korea government MSIP through the National Research Foundation (2013R1A1A2063824, 2015M2B2A4032926, 2015M2B2A9032869 and 2015M2A2A4A01045320).

References

[1] B.F. Gromov, Yu.S. Belomitcev, E.I. Yefimov, M.P. Leonchuk, P.N. Martinov, Yu.I. Orlov, D.V. Pankratov, Yu.G. Pashkin, G.I. Toshinsky, V.V. Chekunov, B.A. Shmatko, V.S. Stepanov, Nucl. Eng. Des. **173**, 207 (1997)
[2] C. Bhatia, J. Adam, V. Kumar, K. Katovsky, M. Majerle, A.A. Solnyshkin, V.M. Tsoupko-Sitnikov, Appl. Radiat. Isot. **70**, 1254 (2012)
[3] O. Svoboda, J. Vrzalová, A. Krása, A. Kugler, M. Majerle, V. Wagner, EPJ Web of Conferences **8**, 07003 (2010)
[4] O. Svoboda, J. Vrzalová, V. Wagner, A. Krása, A. Kugler, M. Majerle, J. Kor. Phys. Soc. **59**, 1709 (2011)
[5] J. Vrzalová, O. Svoboda, A. Kugler, M. Suchopár, V. Wagner, EPJ Web of Conferences **21**, 10007 (2012)
[6] J. Vrzalová, O. Svoboda, A. Krása, A. Kugler, M. Majerle, M. Suchopár, V. Wagner, Nucl. Instr. Meth. Phy. Res. A **726**, 84 (2013)
[7] M.S. Uddin, S. Kamada, M. Hagiwara, T. Itoga, M. Baba, Ann. Nucl. Energy **36**, 1133 (2009)
[8] MC-50 Cyclotron web `http://www.kirams.re.kr/`
[9] J.W. Shin, S.-I. Bak, C.M. Ham, E.J. In, D.Y. Kim, K.J. Min, Y.J. Zhou, T.-S. Park, S.W. Hong, V.N. Bhoraskar, Nucl. Instr. Meth. Phy. Res. A **797**, 304 (2015)
[10] GEANT4 web `http://geant4.web.cern.ch/`
[11] J.W. Shin, T.-S. Park, Nucl. Instr. Meth. Phy. Res. B **342**, 194 (2015)
[12] H. Naik, S.V. Surayanarayana, V.K. Mulik, P.M. Prajapati, B.S. Shivashankar, K.C. Jagadeesan, S.V. Thakare, D. Raj, S.C. Sharma, P.V. Bhagwat, S.D. Dhole, S. Ganesan, V.N. Bhoraskar, A. Goswami, J. Radional. Nucl. Chem. **293**, 469 (2012)
[13] D.Y. Kim, Development of MICROMEGAS and measurements of (n,xn) cross section for fast neutrons Ph. D. Dissertation Sungkyunkwan University Suwon Korea (2014)
[14] TENDL-2009 web `http://www.talys.eu/tendl-2009/`
[15] E. Kim, T. Nakamura, A. Konno, Y. Uwamino, N. Nakanishi, M. Imamura, N. Nakao, S. Shibata, S. Tanaka, Nucl. Sci. Eng. **129**, 209 (1998)